A Review of Berry Curvature, Kubo Formula and The Chern Insulator Model

A course project report to be submitted by

Jabed Umar, Shubhay Dikkar
Roll. No - 2011072, 2011059

School of Physical Sciences
National Institute of Science Education and Research
Jatni, Khurda, Bhubaneswar, 752050, India

Under the supervision of

Dr. Kush Saha

August - November 2023

Abstract

Berry curvature, an essential quantum mechanical concept, has gained considerable attention due to its fundamental role in various physical phenomena, especially in the realm of topological insulators. This work delves into the significance of Berry curvature and its relationship with the Kubo formula, a potent tool in condensed matter physics used to calculate materials' electrical conductivity within the linear response theory framework. Subsequently, we introduce the 2D Chern Insulator Model, highlighting its capacity to exhibit non-trivial insulating states. In a further application, we construct a 3D model by layering 2D planes with different Chern numbers, providing a tangible representation of the layered nature inherent in topological insulators. This model facilitates the calculation of the Chern number in diverse 2D planes within the 3D structure, offering valuable insights into the topological properties of each layer and their intricate interplay in the three-dimensional space.

Contents

1 Introduction

The concept of Berry curvature, discussed in chapter 1, a central idea in quantum mechanics, has garnered substantial attention recently due to its fundamental role in influencing a range of physical phenomena. At the heart of this exploration lies the recognition of Berry curvature as a quantum mechanical quantity that encapsulates geometric information about the evolution of quantum states as they traverse parameter space adiabetically. This unique attribute renders Berry curvature indispensable in understanding and characterizing the behavior of electronic systems, especially those exhibiting topological phases of matter. The interplay between topology and quantum mechanics becomes particularly apparent in the context of topological insulators, where the nontrivial topology of the electronic band structure gives rise to intriguing physical phenomena and novel electronic properties.

Then in the chapter 2, we introduce the concept of Kubo formula, emerges as a powerful analytical tool within the realm of condensed matter physics to calculate the electrical conductivity of materials within the theoretical framework of linear response theory - a key property that governs the flow of electric current in materials. Its integration with Berry curvature is especially noteworthy, as the geometric phase associated with Berry curvature manifests itself in the quantum corrections to the electrical conductivity. This intricate connection underscores Berry curvature's profound impact on materials' macroscopic transport properties.

The project introduces the 2D Chern Insulator Model in chapter 3 , highlighting its band structure and the capacity to exhibit non-trivial insulating states for different parameters of the Model Hamiltonian. Expanding its applicability, a 3D model is formulated in chapter 4 by stacking multiple 2D planes, each characterized by distinct Chern numbers. This layered methodology is a tangible manifestation of the inherent characteristics observed in topological insulators. We study the band structure of the 3D Chern insulators and then compute the Chern number across various 2D planes embedded within the three-dimensional structure. This approach provides valuable insights into the topological properties unique to each layer, illuminating their intricate interplay within the three-dimensional space.

2 Aim of the Project

This project has a dual focus. Firstly, it explores the significance of Berry curvature, a crucial quantum mechanical concept that has garnered considerable attention for its fundamental role in various physical phenomena. The study investigates the relationship between Berry curvature and the Kubo formula, a powerful tool in condensed matter physics employed to calculate materials' electrical conductivity within the linear response theory framework.

Secondly, the project introduces the 2D Chern Insulator Model, emphasizing its ability to manifest non-trivial insulating states. A 3D model is constructed to extend its application by stacking 2D planes with distinct Chern numbers. This layered approach provides a tangible representation of the inherent layered nature found in topological insulators. The 3D model enables the calculation of the Chern number in various 2D planes within the three-dimensional structure, offering valuable insights into the topological properties of each layer and their intricate interplay in the three-dimensional space.

Chapter 1

Review of Berry Curvature

Only a few problems in quantum mechanics are exactly solvable; the Majority of them are solved by assuming non-trivial terms in Hamiltonian as perturbation; depending on the type of perturbation (time-dependent or independent), different approaches are followed to solve the problem. In this section, we will study the quantum mechanics of a system when the perturbation is turned on infinitely slowly so that the eigenstate of the original Hamiltonian continuously evolves into the states of the new Hamiltonian with the same good quantum number. Such processes are called as **Adiabatic**, and depending on the evolution of system parameters, the new eigenstates may acquire an additional phase to that of the trivial dynamic phase called as **Berry's Phase** or **Geometric Phase** which is found to affect the physical property of the system significantly.

1 Berry phase and Winding Number

For a time-dependent perturbation, we can write the Schrodinger equation at an instant of time "t".

$$i\hbar\frac{\partial\left|\psi\right\rangle}{\partial t} = \hat{H}\left|\psi\right\rangle \tag{1.1}$$

Note: The above equation is not the complete Schrodinger equation; it is an equation for **instantaneous eigenstates** of the Hamiltonian. We take the following solution to be our Anstanz[1] and substitute it in the above equation to yield eqn-1.3

$$\left|\psi\right\rangle = \sum_n c_n(t)\left|\phi_{n(t)}\right\rangle \tag{1.2}$$

$$i\hbar\sum_n \partial_t c_n(t)\left|\phi_n(t)\right\rangle + c(t)_n\partial_t\left|\phi_n(t)\right\rangle = \sum_n c_n t E_n(t)\left|\phi_n(t)\right\rangle \tag{1.3}$$

Taking inner product with some other instantaneous eigenstate $\langle\phi_k|$

$$i\hbar\partial_t c_k(t) = c_k(t)E_k(t) - i\hbar\sum_n c_n\bar{\phi_k}\,|\partial_t\phi_n\rangle \tag{1.4}$$

We group the k term in the summation and rewrite the equation

$$i\hbar\partial_t c_k(t) = c_k(t)\{E_k(t) - i\hbar\,\langle\phi_k|\partial_t\phi_k\rangle\} - i\hbar\sum_{n\neq k} c_n\,\langle\phi_k|\partial_t\phi_n\rangle \tag{1.5}$$

The summation becomes negligible if we assume that the states evolve with time so that they don't cross or don't overlap one another with the passage of time. This can happen when states are **Non-degenerate** and are **sufficiently spaced**. The perturbation is turned on very slowly such that change in eigenstates is not appreciable.

$$c_k(t) = c_k(t_o)e^{-\frac{i}{\hbar}\int_{t_o}^{t} E_k(t')dt'}e^{-i\int_{t_o}^{t}\langle\phi_k|\partial_t\phi_k\rangle dt'} \tag{1.6}$$

It can be shown that this extra phase is **purely imaginary** as follows

$$\langle\phi_k|\partial_t\phi_k\rangle = \int \mathbf{dr}\phi_k^*\partial_t\phi_k \rightarrow \frac{d}{dt}\int \mathbf{dr}\phi_k^*\phi_k - \int \mathbf{dr}\phi_k^*\partial_t\phi_k = -\langle\phi_k|\partial_t\phi_k\rangle \tag{1.7}$$

Since eigenstates are normalized, the time derivative of the integral vanishes, proving the purely imaginary nature of the berry phase. The arbitrary wave function of the new Hamiltonian will be of the following form.

$$\psi = \sum_n c_n e^{-i\gamma_n}\phi_n \tag{1.8}$$

In **Parameter space** if the Hamiltonian has form

$$H(\mathbf{R(t)} = H(R_1(t), R_2(t), R_3(t)....R_n(t)) \tag{1.9}$$

Then the berry phase can be expressed in terms of parameters of the Hamiltonian.

$$\frac{d\phi_n(\mathbf{(R(t))})}{dt} = \nabla_R\phi_n(\mathbf{R(t)} \times \frac{d\mathbf{R(t)}}{dt} \tag{1.10}$$

$$\gamma_n = \int_{R_i}^{R_f}\langle\phi_n(\mathbf{R})|\,\nabla\,|\phi_n(\mathbf{R})\rangle\,\mathbf{dr} \tag{1.11}$$

The term inside the integral is called as **Berry Connection** denoted by **A**, which is a vector with n components. **Berry Potential is gauge-dependent**. We can see this by

redefining instantaneous eigenstates as

$$\left|\bar{\psi}_n\right\rangle = e^{-i\beta(R)}\psi_n \tag{1.12}$$

$$\mathbf{A'(R)} = i\left\langle\phi'_n(\mathbf{R})\right|\nabla\left|\phi'_n(\mathbf{R})\right\rangle = i\left\langle\phi_n(\mathbf{R})\right| e^{i\beta(R)}\nabla e^{-i\beta(R)}\left|\phi_n(\mathbf{R})\right\rangle = \nabla_R\beta(\mathbf{R}) + \mathbf{A(R)}$$

$$\mathbf{A'(R)} = \nabla_R\beta(\mathbf{R}) + \mathbf{A(R)} \tag{1.13}$$

The berry phase calculated for this new berry potential will take the following form

$$\gamma'_n = \int_{R_i}^{R_f} A'_n(\mathbf{R}).d(\mathbf{R}) = \gamma_n(R) + \beta(\mathbf{R}_f) - \beta(\mathbf{R}_i) \tag{1.14}$$

If $R_i = R_f$, we can argue that it returned into the same eigenstates as earlier, which implies.

$$e^{-i\beta(R_i)} = e^{-i\beta(R_f)} \tag{1.15}$$

This is generally satisfied if

$$\beta(R_f) = \beta(R_i) + 2\pi m \tag{1.16}$$

This suggests that under a cyclic process, the eqn-1.14 transforms into the following equation

$$\gamma' = \gamma + 2\pi m \tag{1.17}$$

The m appearing in the above two equations is called as **Winding number**[4,5,7]. Since $e^{i\beta}$ is a complex number lying on a unit circle on an Agrand plane, the number m physically represents the number of times it has traced/winded the circle, hence the name winding number. This number can be used to classify the gauge transformation.

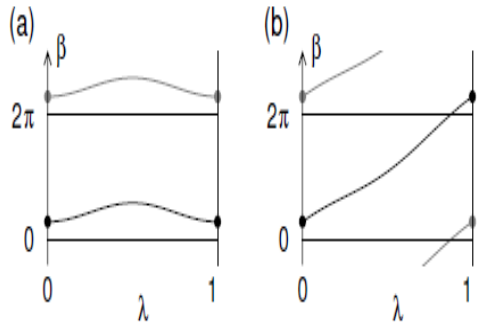

Figure 1.1: (a)Progressive Transformation, (b)Radical Transformation

When m=0, the gauge is like Fig. 1.1 (a). It is smoothly deformed over the interval transformation, while for non-trivial m, it is a discontinuous jump of height 2π.

2 Berry Curvature and Chern Theorem

In the earlier section, we expressed the berry phase in terms of Berry potential, which is a Gauge dependent quantity, we will use the **stokes theorem** to express it in a gauge-independent quantity called as **Berry Curvature**

$$\gamma_n = \oint A_n(R).dR = \oint \Omega_n(R).dS \tag{1.18}$$

In vectorial notation

$$B_i = \epsilon_{ijk}\partial_j A_k = i\epsilon_{ijk}\partial_j \langle\phi|\partial_k\phi\rangle \tag{1.19}$$

Since there is an "i" in the definition of Berry potential, we can write the berry curvature as an Imaginary part of the above quantity without the "i" term. Further, the derivative ∂_j can be taken inside the integral as the component over with integration is being carried out is different than it. After going inside, it will differentiate the inner product according to the chain rule, leading us to the following formula.

$$\Omega_{n,jk} = -2Im\,\langle\partial_j\phi|\partial_k\phi\rangle \tag{1.20}$$

Expanding the above term by putting the outer product inside the inner product, we get

$$\Omega_{n,jk} = -2Im\sum_{n'}\langle\partial_j\phi_n|\phi_{n'}\rangle\,\langle\phi_{n'}|\partial_k\phi_n\rangle \tag{1.21}$$

By differentiating the Schrodinger equation with respect to a parameter and rearranging the terms, we will yield the following relation.

$$\langle\phi_{n'}|\partial_k\phi_n\rangle = -2Im\frac{\langle\phi_{n'}|\,\partial_k H\,|\phi_n\rangle}{(E_n - E_{n'})^2} \tag{1.22}$$

Using this relation in eqn-1.21 will yield the summation formula commonly used to calculate berry curvature in a system numerically [4,8].

$$\Omega_{n,jk} = -2Im\sum_{n'\neq n}\frac{\langle\phi_n|\,\partial_j H\,|\phi_{n'}\rangle\,\langle\phi_{n'}|\,\partial_k H\,|\phi_n\rangle}{(E_n - E_{n'})^2} \tag{1.23}$$

Symmetries and Berry Curvature

We will see in the upcoming chapters that the presence of finite Berry curvature is of utmost importance for topological properties to arise. This quantity is calculated by integrating the berry curvature over the k space, and symmetries like time-reversal

symmetry and inversion symmetry establish restrictions on berry curvature when present. Generally, it depends on the symmetries of the material under study, which preserves or vanishes certain berry curvature components in the k space as berry curvature is a vector in k space. A normal transformation matrix for vectors can be used to transform it.For e.g in Mn_3Sn the presence of $M_y|\tau_{c/2}$ makes only Ω_{xz} to be finite. Here we will discuss two important symmetries **Inversion Symmetry** and **Time Reversal symmetry**

- **Inversion Symmetry:**If the material is Centrosymmetric, then the symmetry's Hamiltonian commutes with the inversion operator.

$$[P, H] = 0 \tag{1.24}$$

  Here P is inversion operator,Hence $\phi(-k) = \phi(k)$,thus it leads to $\Omega(k) = \Omega(-k)$ using eqn(1.23)

- **Time reversal symmetry:**A time reversal operator is an anti-unitary operator of the form the UK, U is a unitary operator, and K is a complex conjugation operator. For spinor, it takes the following form

$$T = i\sigma_2 K \tag{1.25}$$

  This comes due to the fact that J changes sign under time reversal; for a system having a Time reversal system, it should satisfy

$$TH = HT \tag{1.26}$$

  From the **Krammer's Theorem**(see appendix), we have $T\,|\phi_{n,-k}\rangle = \phi_{n,k}$, here parameter is taken to be momentum which the case for lattice. Now, as Time reversal operator is anti-unitary we can write

$$T^\dagger T = K \tag{1.27}$$

  Inserting this in the inner product of eqn(1.20) yields us

$$\Omega_{n,jk'}(-k) = -2Im\,\langle\partial_j\phi(-k)|\partial_{k'}\phi(-k)\rangle \tag{1.28}$$

$$= -2Im\,\langle\partial_j\phi(k)|\,T^\dagger T\,|\partial_{k'}\phi(k)\rangle$$

$$= -2Im\,\langle\partial_j\phi(k)|\,K\,|\partial_{k'}\phi(k)\rangle = 2Im\,\langle\partial_j\phi(k)|\,K\,|\partial_{k'}\phi(k)\rangle$$

$$= -\Omega_{n,jk'}(k)$$

Thus, we can see if a system has both Time reversal symmetry and inversion symmetry, then the berry curvature will be zero at each site. Hence, breaking of TRS is crucial to observe topological phenomena.

Chern Theorem

It states that the surface integral of berry curvature over any closed 2D manifold is 2π times an integer, which is called as **chern number** or **Topological invariant**

$$\oint \Omega \mathbf{dS} = 2\pi m \tag{1.29}$$

Proof: Consider a sphere divided into parts by the curve C; for the top part, A, the line integral is clockwise and for part B, the line integral is anticlockwise; hence, there will be a negative sign on the surface integral for the case of anticlockwise rotation.

$$\oint_{Ca} A.\mathbf{dR} = \oint_{a} \Omega.\mathbf{dS} + 2\pi m_1, \oint_{Cb} A.\mathbf{dR} = -\oint_{b} \Omega.\mathbf{dS} + 2\pi m_2 \tag{1.30}$$

but since the value of both the line integral must be the same, by equating the above two equations, we get.

$$\oint_{a} \Omega.\mathbf{dS} + \oint_{b} \Omega.\mathbf{dS} = \oint \Omega.\mathbf{dS} = 2\pi m \tag{1.31}$$

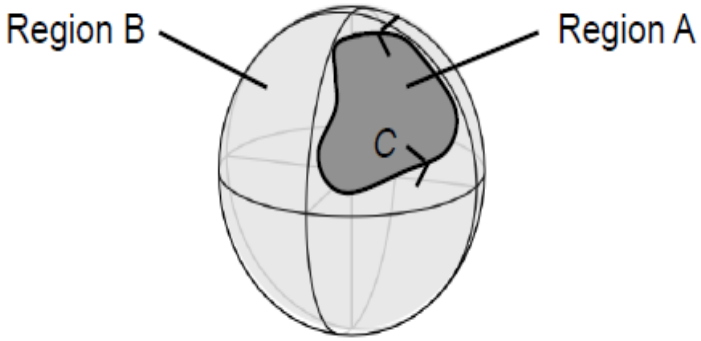

Figure 1.2: Berry curvature is calculated over the sphere integration

3 Berrylogy of Brillouin zone

The Hamilton for a single electron in a crystal is given as follows within the independent electron approximation.

$$\hat{H} = \frac{\hat{p}^2}{2m} + V \tag{1.32}$$

where V(r) = V(r+R) and R is the Primitive lattice vector, the solution of this equation comes from the Bloch's Theorem

$$\psi_{nk} = e^{ik.r} u_{nk}(r) \tag{1.33}$$

Due to cell periodicity, Bloch wave functions are restricted to

$$\psi_{nk}(r + R) = e^{ik.r} \psi_{nk}(r) \tag{1.34}$$

thus, the boundary condition depends on k, which is not easy to deal with in the calculation of berry curvature; our Hamiltonian is k independent; we can transform our Hamiltonian in k space in the following way: suppose we want to get the expectation value of H then

$$\langle \psi_{nk} | \hat{H} | \psi_{nk} \rangle = \langle u_{n,k} | e^{-ik.r} \hat{H} e^{ik.r} | u_{n,k} \rangle \tag{1.35}$$

Further, the Hamiltonian changes to

$$\hat{H}_k = e^{-ik.r} \hat{H} e^{ik.r} = \frac{(\hat{p} + \hbar k)^2}{2m} + V \tag{1.36}$$

Here $\hbar k$ is called crystal momentum in solid, and $u_{n,k}$ are the cell periodic part of the Bloch wave function. This shows that the cell periodic shall be used in calculating berry phase and berry curvature in solids rather than the Bloch wave function.

$$\Omega_{n,k} = \nabla \times i \langle u_{n,k} | \nabla | u_{n,k} \rangle \tag{1.37}$$

For a 1D lattice with a lattice parameter 'a' the Brillouin zone is between $\frac{-\pi}{a}$ to $\frac{\pi}{a}$ since $u_{nk}(r)$ are periodic within the Brillouin zone thus the band structure can be best viewed as a cylinder where the periodicity is of $(2\pi)/a$ then the berry phase in context of lattice is termed as **Zak phase**

$$\gamma_n = \oint \Omega_{n,k} d^3k \tag{1.38}$$

For the berry phase to be defined, we need $\psi_{n,k}(r)$ to be smoothly varying; thus, at k= 0 and k = $2\pi/a$, its value should be the same, but since berry phase in the lattice is computed using the cell function of bloch states which put the following condition.

$$u_{n,k=2\pi/a}(r) = e^{-i2\pi x/a} u_{n,k=0} \tag{1.39}$$

This extra phase factor is essential in calculating the berry phase for a 1D system. To compute the berry phase in 1 D lattice, we discrete the Brillouin zone into N intervals and

compute $u_{n,ki}$ for $i = 0, ..., N-1$with $k_i = 2\pi i/N$..We know the berry phase is acquired by an eigenstate over a closed loop in parameter space. If we discrete the parameter space, calculate the phase difference between each nearing state and sum them up over a path, we should get the berry phase as follows.

$$\gamma_n = arg(\langle\phi_0|\phi_1\rangle \langle\phi_1|\phi_2\rangle \langle\phi_2|\phi_3\rangle ..... \langle\phi_{N-1}|\phi_0\rangle) \tag{1.40}$$

In 1D lattice, this takes the following form where we use eqn(1.39) to fix the N state[7,8]

$$\gamma_n = arg(\langle u_{nk0}|u_{nk1}\rangle \langle u_{nk_1}|u_{nk2}\rangle \langle u_{nk2}|u_{nk3}\rangle ..... \left\langle u_{nk(N-1)}\right| e^{-i2\pi x/a} |u_{nk0}\rangle) \tag{1.41}$$

In the 2D system, the parameter space will be two-dimensional, and their Brillouin zone will also be a square in k space; hence the summation will look like the following. Let us assume that in our BZ, there are N and M values, respectively, in the x and y direction

$$\gamma_n = arg(\sum_{n=1}^{N-1} \tau(n,1)(n{+}1,1){+}\sum_{m=1}^{M-1} \tau(1,m)(1,m{+}1){+}\sum_{n=1}^{N-1} \tau(n,M)(n{+}1,M){+}\sum_{m=1}^{N-1} \tau(N,m{+}1)(N,M))$$

For example, the band structure is a circle in the 1D case. For 2D, it is a 2-dimensional torus; for 3D, it is 3 3-dimensional torus. The above algorithm is also true for 3D cases. As for 3D, we calculate the berry phase by fixing one plane so the effective Brillouin zone becomes a square. Once the Berry phase is calculated, we can calculate the chern number by dividing it by 2π

$$C_n = \frac{\gamma_n}{2\pi} \tag{1.42}$$

Chapter 2

Electrical Conductivity

1 Anomalous Hall Conductivity

Let O be any physical operator then rate of change in its expectation value with respect to some parameter λ is given as

$$\partial_\lambda \langle O \rangle = \langle \partial_\lambda n | \, O \, | n \rangle + \langle n | \, O \, | \partial_\lambda n \rangle = 2Re \, \langle n | \, O \, | \partial_\lambda n \rangle \tag{2.1}$$

After hitting the solution of sternhiemer equation(Appendix-1) with $\langle n|$ we get

$$\langle n | \, O \, | \partial_\lambda n \rangle = -iA_n + \langle n | \, OT_n(\partial_\lambda H) \, | n \rangle \tag{2.2}$$

Since A is always real we get the final equation of the form,we get the Q_n in expression by using eqn-6.9 of appendix.

$$\partial_\lambda \langle O \rangle = 2Re \sum_n^{Occ.} \langle n | \, OQ_n \, | \partial_k n \rangle \tag{2.3}$$

We can express it in continuous form as follows

$$\partial_\lambda \langle O \rangle = \frac{V}{(2\pi)^3} \sum_n^{Occ.} 2Re \int_{Bz} \langle n | \, OQ_k \, | \partial_k n \rangle \, d^3k \tag{2.4}$$

For a lattice rather than Bloch eigenfunction their cellular part is taken in calculation for reason explained in chapter One.

$$\frac{\partial_\lambda \langle O \rangle}{V} = \frac{1}{(2\pi)^3} \sum_n^{Occ.} 2Re \int_{Bz} \langle u_{n.k} | \, OQ_k \, | \partial_k u_{n,k} \rangle \, d^3k \tag{2.5}$$

Since the above equation is summing the inner product value over all possible values its natural to introduce Fermi distribution if the system is not at zero Kelvin.

$$\frac{\partial_\lambda \langle O \rangle}{V} = \frac{1}{(2\pi)^3} \sum_n^{Occ.} 2Re \int_{Bz} f_{n,k} \langle u_{n.k} | OQ_k | \partial_k u_{n,k} \rangle \, d^3k \tag{2.6}$$

In our case we will assume the system to be at 0k and use the eqn-2.5 instead to derive the conductivity relation in **2 Dimensional system** where it is slightly modified into

$$\frac{\partial_\lambda \langle O \rangle}{V} = \frac{1}{(2\pi)^2} \sum_n^{Occ.} 2Re \int_{Bz} \langle u_{n.k} | OQ_k | \partial_k u_{n,k} \rangle \, dk \tag{2.7}$$

Digression

1)From the Ohms law we have J = σ E this is where we assume our material is Ohmic

$$\sigma_{\mu\nu} = \frac{\partial J_\nu}{\partial E_\mu} = \frac{1}{V} \partial_\mu (-e v_\nu) \tag{2.8}$$

Thus we get an idea that our operator in eqn(2.7) should be $-ev_\nu$.

2)Another useful relation between v,r and Q can be derived by noting the velocity operator in solid is $v_K = -i/\hbar[r, H_k]$ which yeild eqn(2.9) after operning the commutator

$$\langle u_{m,k} | v_K | u_{n,k} \rangle = \frac{-i}{\hbar} \langle u_{m,k} | r | u_{n,k} \rangle (E_{n,k} - E_{m,k}) \tag{2.9}$$

$$\langle u_{m,k} | r | u_{n,k} \rangle = i\hbar \frac{\langle u_{m,k} | v_K | u_{n,k} \rangle}{E_{n,k} - E_{m,k}} \tag{2.10}$$

Multiplying both sides of Eq. (2.9) on the left by $\langle u_{m,k}|$ and summing over all unoccupied bands m then yields

$$Q_n r | u_{n,k} \rangle = i\hbar T_{n,k} v_K | u_{n,k} \rangle \tag{2.11}$$

3)Using the above relation we can derive another relation using sternhiemer equation.

$$Q_k | \partial_\mu u_{n,k} \rangle = -eT_{n,k} r_\mu | u_{n,k} \rangle \tag{2.12}$$

Here we have taken our H to be of form -eE.r ,Practically actual Hamiltonian may have some other prefactors but this is the most general form for H where electric field is applied to the system.Since $Q_k^2 = Q_k$ we can rewrite the above equation as

$$Q_k^2 | \partial_\mu u_{n,k} \rangle = -eT_{n,k} Q_k r_\mu | u_{n,k} \rangle \tag{2.13}$$

Using eqn(2.11) we get.

$$Q_k^2 \left|\partial_\mu u_{n,k}\right\rangle = i\hbar e T_{n,k}^2 v_\mu \left|u_{n,k}\right\rangle \tag{2.14}$$

Which is same as saying

$$Q_k \left|\partial_\mu u_{n,k}\right\rangle = i\hbar e T_{n,k}^2 v_\mu \left|u_{n,k}\right\rangle \tag{2.15}$$

4)We make use of one another trick involving the velocity operator namely we now

$$\partial_k H_k = \hbar v_k \tag{2.16}$$

Now we can put this in eqn(6.9) and changing the eigenstates to cellular part of Bloch eigenstates we get

$$Q_k \partial_\mu u_{n,k} = \hbar T_{n,k} v_{\mu,k} u_{n,k} \tag{2.17}$$

Here ∂_μ is $\partial/\partial k_\mu$, Relation (2.17,2.15,2.11,2.8) will help us deriving the conductivity formula.

We can now substitute eqn(2.15) in eqn(2.7) by taking operator to be $-ev_\mu$

$$\sigma_{\mu,\nu} = -\frac{e^2\hbar}{(2\pi)^2} \sum_n^{Occ.} 2Im \int_{Bz} \left\langle u_{n,k}\right| v_{\mu,k} T_{n,k}^2 v_{\nu,k} \left|u_{n,k}\right\rangle \tag{2.18}$$

We can see for $\mu = \nu$ the inner product becomes real hence σ_{xx}, σ_{yy} are both zero ,In general we can use the eqn(2.17) to rewrite the equation as

$$\sigma_{\mu,\nu} = -\frac{e^2}{(2\pi)^2\hbar} \sum_n^{Occ.} 2Im \int_{Bz} \left\langle \partial_\mu u_{n,k}\right| Q_n^2 \left|\partial_\nu u_{n,k}\right\rangle d^2k \tag{2.19}$$

Since Q_n^2 is same as Q_n,further Q_n is 1 - $\left|n\right\rangle \left\langle n\right|$,

$$\sigma_{\mu,\nu} = -\frac{e^2}{(2\pi)^2\hbar} \sum_n^{Occ.} 2Im \int_{Bz} \left\langle \partial_\mu u_{n,k}|\partial_\nu u_{n,k}\right\rangle d^2k \tag{2.20}$$

Here the contribution from $\left|n\right\rangle \left\langle n\right|$ will vanish because those terms are real.Now we can use the definition of Berry curvature

$$\Omega_{n,\mu\nu} = \partial_\mu A_{n,\nu}(k) - \partial_\nu A_{n,\mu}(k) = -2Im \left\langle \partial_\mu u_{n,k}|\partial_\nu u_{n,k}\right\rangle \tag{2.21}$$

Hence we get the **Anomalous Conductivity** equation for 2-D case as follows.

$$\sigma_{\mu,\nu} = \frac{e^2}{(2\pi)^2\hbar} \sum_{n}^{Occ.} \int_{Bz} \Omega_{n,\mu\nu} d^2k \tag{2.22}$$

If for a 2-D system k space form a torus then integral will become cyclic then we can express Integral over berry curvature as chern number giving us the final result,

$$\sigma_{\mu,\nu} = \frac{e^2}{h} \sum_{n}^{Occ.} C_n \tag{2.23}$$

This relation was originally derived by D. J. Thouless et al. (1982) in the context of the integer quantum Hall effect in the presence of a periodic potential This could be generalised to 3-D system as follows

$$\sigma_{\mu,\nu} = \frac{e^2}{(2\pi)^3\hbar} \sum_{n}^{Occ.} \int_{Bz} f_{n,k} \Omega_{n,\mu\nu} d^3k \tag{2.24}$$

eqn(2.24) is the **Anomalous conductivity formula**,this suggest that for a material with finite berry curvature it can give rise to transverse voltage without application of any magnetic field this effect is called as **Anomalous Hall effect**.

2 Role of Spin-Orbit Coupling

Haldane model is considered as the earliest model for 2D topological insulator which dates back to 1968 but only recently in 2013 it was experimentally realised in Cr doped Bi_2Te_3,it was due to non-trivial constrains supported by theory on class of material that can show this phenomena.Generally a topological insulator differs from a trivial insulator by a occurrence of a semi metallic states under continuous deformation of Hamiltonian.Putting it simply for a state is topological if its connected to a trivial states under a few parameter changes in Hamiltonian by a semi metallic state occurring in between.This states are characterized by Chern number ,For a trivial state it is always zero its similar to that of genus in real solids,Two different topological state can only be distinguished if they have different topology.Thus making an analogy to the real system a manifold in space is like a surface and berry curvature is like a real curvature in real space.The important condition for a material to show topological properties apart from being 2 dimensional,Insulating are as follows

- **Presence of Magnetization :**This arises since we need the integral over berry curvature to be finite for which Time Reversal Symmetry must be broken one way in which it can be broken is due to Magnetization perpendicular plane.This is hard to realise experimentally because most of ferromagnetic material are not insulator

- **Presence of Strong SOC :** Due to absence of Spin Orbit coupling both up spin and down spin Hamilton are real for a system hence it commutes with a complex conjugation operator (K) ,and as $\hat{T} = \hat{U}\hat{K}$ thus it has a time reversal symmetry its the SOC which breaks the TRS,The magnitude of gap depends on the strength of Spin orbit coupling hence we need the material to show high spin orbit coupling hence a atoms with Z greater than 50 are required in material

Practically this condition can't be satisfied but unconventional ways can be used to escape from this trap like Non-co planar spin arrangements decouple the spin up and down moments in a way similar to SOC thus breaks the TRS indirectly,other ways are strong correlation (Correlation are one body operator terms used in DFT they represent non-classical many body effects in solids,so if the correlation in our Hamilton take a form in way that it effectively breaks the TRS).The Cr doped Bi_2Te_3 works in similar way its based on a theory paper proposed by Yu et al. (2010) in which it is shown that how magnetic impurities(Cr) doped on a Van Vleck paramagnetic material(Bi_2Te_3) can give rise to a long range ferromagnetic interaction that breaks the TRS and open up the gap in the system.

Chapter 3

2D Chern Insulator Model

Band insulators, characterized by a fully occupied valence band and an unoccupied conduction band, feature a substantial energy gap that hinders the flow of electrical charge. Chern insulators are a captivating class of two-dimensional materials within this category, showcasing distinctive electronic properties attributable to their nontrivial topological order. The term "Chern insulator" is linked to the Chern number, a topological invariant delineating the electronic band structure of these materials.

To elucidate the principles behind Chern insulators, we employ the QWZ model [2], a conceptual framework introduced by Qi, Wu, and Zhang. In our exploration, we extend the model by introducing an additional parameter to parameterize the hopping behaviour.

1 Model Hamiltonian and Energy Bands:

The bulk Hamiltonian of the 2D system with non-vanishing Chern number is given by

$$H(k_x, k_y) = \sin k_x \cdot \sigma_x + \sin k_y \cdot \sigma_y + [m - 2t(\cos k_x + \cos k_y)] \cdot \sigma_z \tag{3.1}$$

The eigenvalues of the given Hamiltonian are (see Appendix 2)

$$E_\pm = \pm\sqrt{\sin^2 k_x + \sin^2 k_y + [m - 2t(\cos k_x + \cos k_y)]^2} = \pm|d(k)| \tag{3.2}$$

Since the band closing condition requires $\pm|d(k)| = 0$, i.e the band closing conditions are

1. $\frac{m}{t} = 4$ at $k_x = 0$ & $k_y = 0$
2. $\frac{m}{t} = 0$ at $k_x = 0$ & $k_y = \pi$ or $k_x = \pi$ & $k_y = 0$
3. $\frac{m}{t}$ = -4 at $k_x = \pm\pi$ & $k_y = \pm\pi$

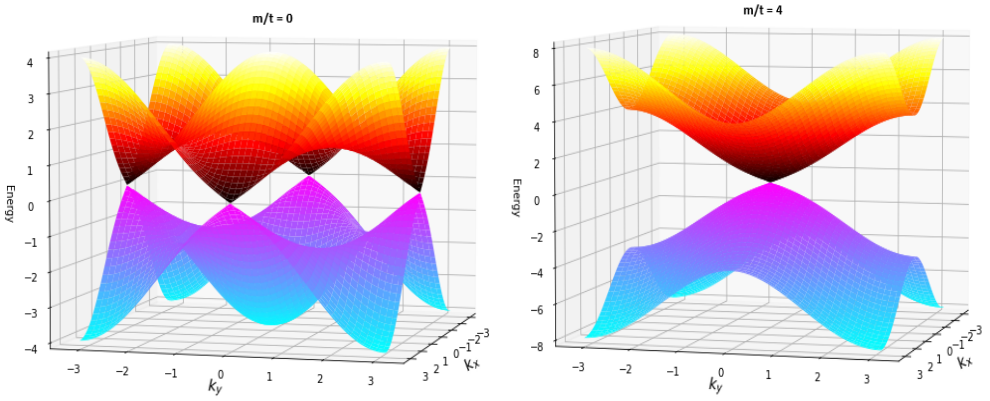

Figure 3.1: Band Structure for $\frac{m}{t} = 0$ and $\frac{m}{t} = 4$

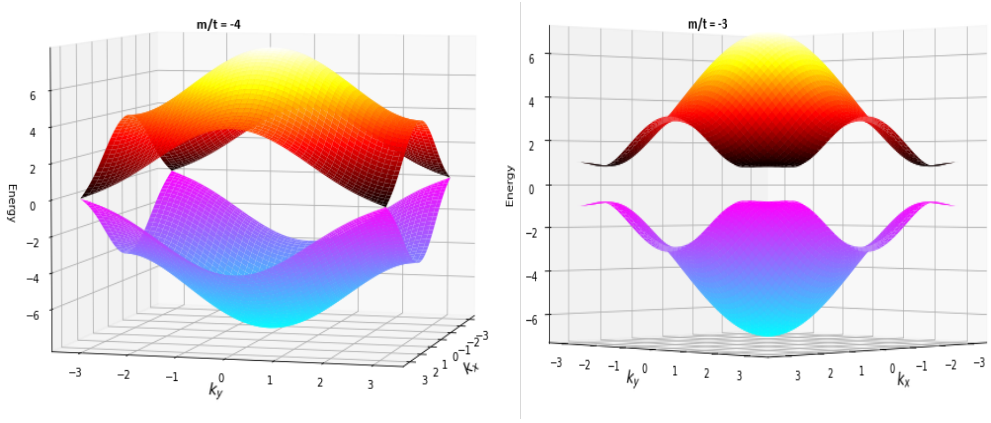

Figure 3.2: Band Structure for $\frac{m}{t}$ = -4 and $\frac{m}{t}$ = -3

In the vicinity of a gap closing point, called Dirac point [3], the dispersion relation has the shape of a Dirac cone, as seen in Fig. 3.1 & 3.2. For all other values of $\frac{m}{t} \neq 0$, -4, 4, the spectrum is gapped. Therefore, it is meaningful to explore the system's topological properties. The system demonstrates insulating behaviour when the ratio $\frac{m}{t}$ assumes a generic value such as -3.

2 Chern Number of the Model Hamiltonian:

The Chern number is a topological invariant that quantifies the nontrivial topology of electronic band structures in materials. It is especially crucial in studying Chern insulators, providing a numerical descriptor for their unique topological properties, such as quantized Hall conductance[4] and the presence of chiral edge states[7]. A brief on Chern number calculation can be found in Chapter 1.

The Hamiltonian can be written as H $(k_x, k_y) = \vec{d}(k_x, k_y) \cdot \vec{\sigma}$. The corresponding $\vec{d}(k_x, k_y)$

can be written as

$$\vec{d}(k_x, k_y) = \begin{pmatrix} \sin k_x \\ \sin k_y \\ m - 2t(\cos k_x + \cos k_y) \end{pmatrix} = \begin{pmatrix} d_x \\ d_y \\ d_z \end{pmatrix}$$

Let's discuss an alternative method for computing the Chern Number of the system. The graphical approach involves counting the number of times the torus, formed by the image of the Brillouin zone in the space of $\vec{d}(\mathbf{k})$, encloses the origin. To gain insight into the non-trivial geometry of the torus, it is illuminating to observe a gradual sweep of the Brillouin zone (refer to the figure below).

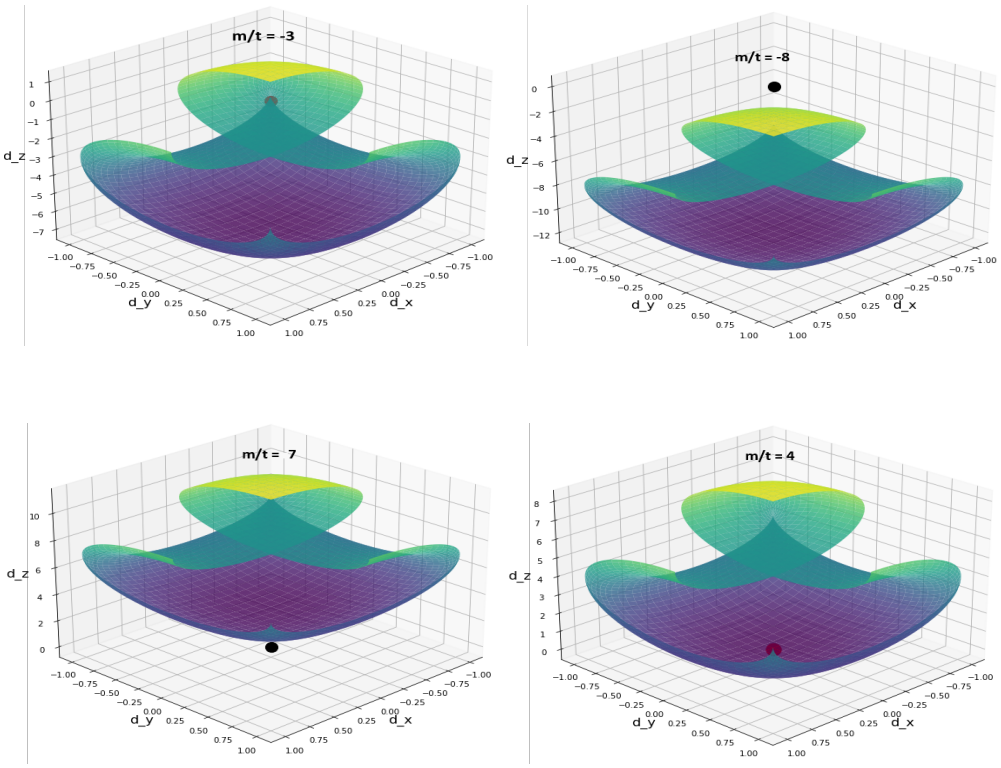

Figure 3.3: The surface $\vec{d}(\mathbf{k})$ as $\mathbf{k}$ varies over the interval $(-\pi, \frac{\pi}{2})$ for various values of $\frac{m}{t}$.

For values of $\frac{m}{t} < -4$ and $\frac{m}{t} > 4$, the curve does not wind or enclose the origin. In such cases, the Chern number of the system is zero. The two bands touch when $\frac{m}{t}$ takes on the values $0, \pm 4$. The Chern number is ill-defined at these points, and the curve touches the origin.

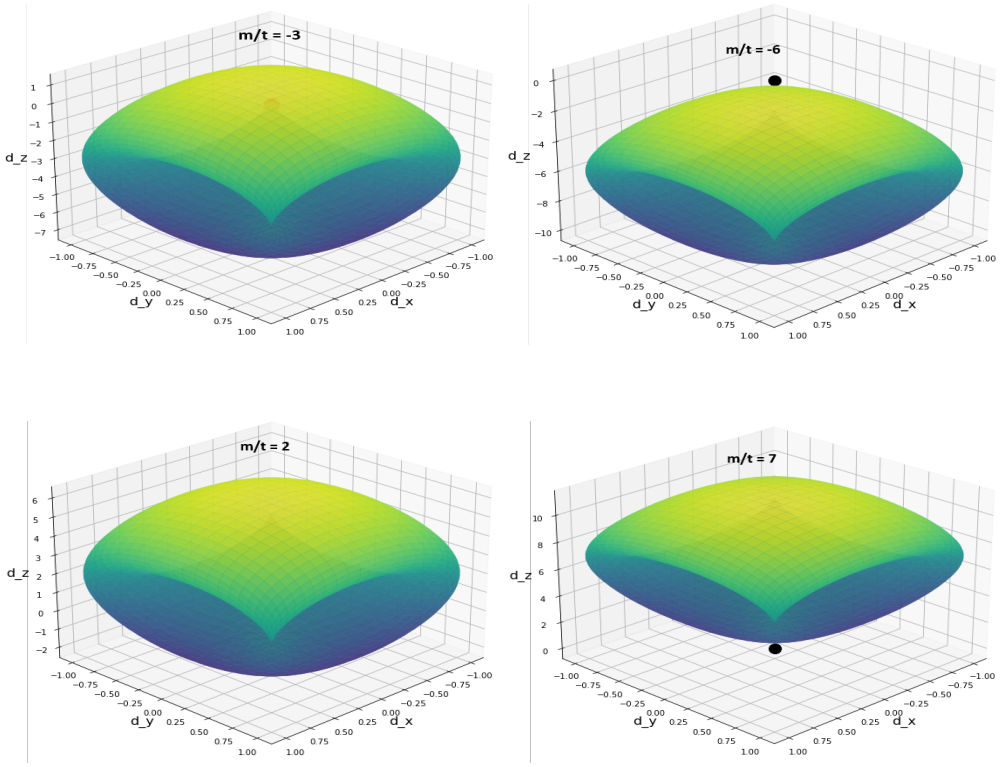

Figure 3.4: The surface $\vec{d}(\mathbf{k})$ as $\mathbf{k}$ varies over the entire BZ for various values of $\frac{m}{t}$.

When exploring the entire Brillouin zone (BZ) by varying the wave vector $\vec{k}$, a notable phenomenon emerges: the parameter $\frac{m}{t}$ orchestrates a systematic shift of the entire torus along the d_z direction. This adjustment allows us to control whether the torus encapsulates the origin dynamically. Three distinct scenarios unfold within our model, each elucidated in the accompanying figure.

Firstly, for extreme values of $\frac{m}{t}$, such as -6 and 7, the torus does not encompass the origin, resulting in a Chern number (Q) of 0. This particular configuration prevails when $\frac{m}{t}$ surpasses 4.

Secondly, an intriguing scenario arises when the origin lies within the torus. In this case, a line extending from the origin to infinity inevitably intersects the torus. If $\frac{m}{t}$ falls within the range of -4 to 0, the initial intersection occurs from the green side (outer side) of the surface, yielding a Chern number of -1 (as in $\frac{m}{t}$ = -3 case). Conversely, for $\frac{m}{t}$ in the range of 0 to 4, the intersection is from the blue side (inner side) of the surface, resulting in a Chern number of 1 (as in $\frac{m}{t} = 2$ case).

To demonstrate the last point, we specifically explore the Brillouin zone (see figure below) with k_x values in the range $(-\pi, \frac{\pi}{2})$ and k_y values spanning $(-\pi, \pi)$. In instances where $0 < \frac{m}{t} < 4$, the initial intersection of the torus occurs from the blue side (inner side) of the surface, exemplified by the case when $\frac{m}{t} = 3.4$. Conversely, when $-4 < \frac{m}{t} < 0$, the

torus is initially intersected from the green side (outer side) of the surface, as observed in the case of $\frac{m}{t}$ = -3.

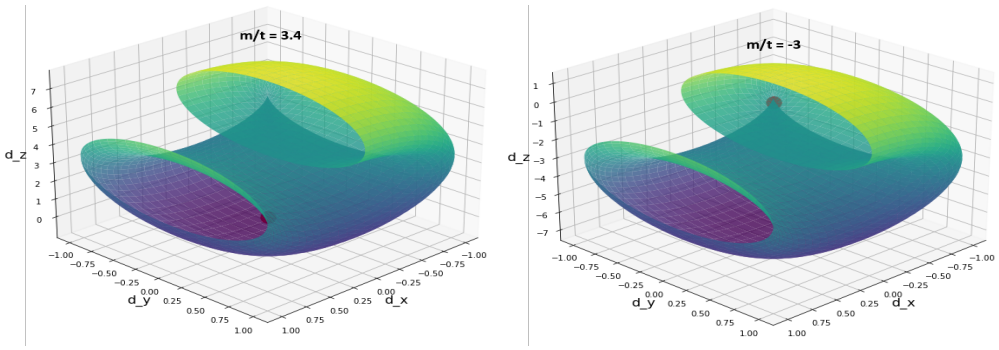

Figure 3.5: The surface $\vec{d}(\mathbf{k})$ with $k_x \rightarrow (-\pi, \frac{\pi}{2})$ and $k_y \rightarrow (-\pi, \pi)$ for $\frac{m}{t}$ = 3.4 & -3.

In summary, the Chern Number and nature of the model's spectrum for different ranges of $\frac{m}{t}$ are as follows:

1. $\frac{m}{t} < -4$: $Q = 0$, indicating an insulating state with a gapped spectrum.

2. $\frac{m}{t} = -4$: Q is ill-defined, and the spectrum exhibits two band touches at four points, characterizing a semi-metallic state.

3. $-4 < \frac{m}{t} < 0$: $Q = -1$, signifying an insulating state with a gapped spectrum.

4. $\frac{m}{t} = 0$: Q is ill-defined, and the spectrum features two band touches at four points, indicative of a semi-metallic state.

5. $0 < \frac{m}{t} < 4$: $Q = 1$, pointing to an insulating state with a gapped spectrum.

6. $\frac{m}{t} = 4$: Q is ill-defined, and the spectrum displays two band touches at one point, reflecting a semi-metallic state.

7. $\frac{m}{t} > 4$: $Q = 0$, indicating an insulating state with a gapped spectrum.

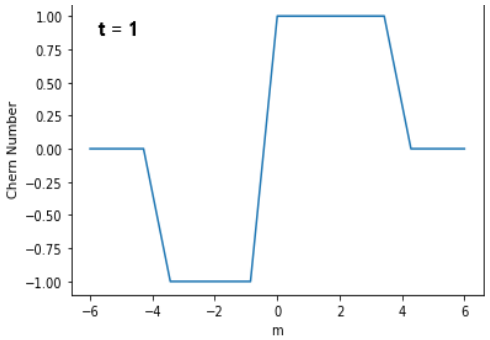

Figure 3.6: Chern Number as a function of m

The transition between metallic and insulating states in the system can be elucidated by examining the Chern number of the lower band plotted against the ratio $\frac{m}{t}$, as depicted

in the above graph. Notably, the sign change in the Chern number corresponds to a shift in the system's state from metallic to insulating. This transition occurs whenever $|\frac{m}{t}| < 4$ indicates that the system exhibits topological characteristics in this regime.

3 Real Space Hamiltonian :

The real space Hamiltonian of our model Hamiltonian can be obtained using the inverse Fourier transformation. The Full Hamiltonian of the system is

$$H(k_x, k_y) = \sum_{k_x,k_y} \sin k_x \cdot \sigma_x + \sin k_y \cdot \sigma_y + [m - 2t(\cos k_x + \cos k_y)] \cdot \sigma_z = \sum_{k_x,k_y} H(\mathbf{k})$$

The real space Hamiltonian is

$$H(x, y) = \sum_{k_x,k_y} C^{\dagger}_{k\uparrow}(\sin k_x \cdot \sigma_x + \sin k_y \cdot \sigma_y + [m - 2t(\cos k_x + \cos k_y)] \cdot \sigma_z)C_{k\downarrow} \tag{3.3}$$

Since the Hamiltonian has translational symmetry in both directions. i.e by using the Fourier expansion of the $C^{\dagger}_{k\uparrow}$ and $C_{k\downarrow}$

$$H(x, y) = \sum_{k_x,k_y} \sum_{x,y,x\prime,y\prime} e^{ik_x x + ik_y y} C^{\dagger}_{x,y} H(k) e^{-ik_x x\prime - ik_y y\prime} C_{x\prime,y\prime}$$

The first term will be of the form

$$H_1(x, y) = \sum_{k_x,k_y} \sum_{x,y,x\prime,y\prime} e^{ik_x x + ik_y y} C^{\dagger}_{x,y} \sin k_x \sigma_x e^{-ik_x x\prime - ik_y y\prime} C_{x\prime,y\prime}$$

$$= \sum_{k_x,k_y} \sum_{x,y,x\prime,y\prime} \sigma_x e^{ik_x x + ik_y y} C^{\dagger}_{x,y} \left(\frac{e^{ik_x} - e^{-ik_x}}{2i} \right) e^{-ik_x x\prime - ik_y y\prime} C_{x\prime,y\prime}$$

$$= \sum_{k_x,k_y} \sum_{x,y,x\prime,y\prime} (\frac{\sigma_x}{2i}) \left(e^{ik_y(y-y\prime)} e^{ik_x(x-x\prime+1)} - e^{ik_y(y-y\prime)} e^{ik_x(x-x\prime-1)} \right) C^{\dagger}_{x,y} C_{x\prime,y\prime}$$

After using the definition of the delta function in exponential form,

$$= \sum_{x,y,x\prime,y\prime} (\frac{\sigma_x}{2i}) \left(\delta(y - y\prime)\delta(x - x\prime + 1) - \delta(y - y\prime)\delta(x - x\prime - 1) \right) C^{\dagger}_{x,y} C_{x\prime,y\prime}$$

After simplification, the 1st term will be of the form,

$$H_1(x,y) = \sum_{x,y}(\frac{\sigma_x}{2i})\left(C^\dagger_{x,y}C_{x+1,y} - C^\dagger_{x+1,y}C_{x,y}\right) \tag{3.4}$$

Similarly, the 2nd term will be of the form

$$H_2(x,y) = \sum_{x,y}(\frac{\sigma_y}{2i})\left(C^\dagger_{x,y}C_{x,y+1} - C^\dagger_{x,y+1}C_{x,y}\right) \tag{3.5}$$

And the 3rd term will be

$$H_3(x,y) = \sum_{x,y}(m\sigma_z)C^\dagger_{x,y}C_{x,y} - [t\sigma_z\left(C^\dagger_{x,y}C_{x,y+1} + h.c\right) + \left(C^\dagger_{x,y}C_{x,y+1} + h.c\right)] \tag{3.6}$$

Therefore, the total real space Hamiltonian will be

$$H(x,y) = \sum_{x,y}(m\sigma_z)C^\dagger_{x,y}C_{x,y} + (\frac{\sigma_x}{2i} - t\sigma_z)C^\dagger_{x,y}C_{x+1,y} + (\frac{\sigma_y}{2i} - t\sigma_z)C^\dagger_{x,y}C_{x,y+1} + h.c$$

Pictorially, the real space Hamiltonian is,

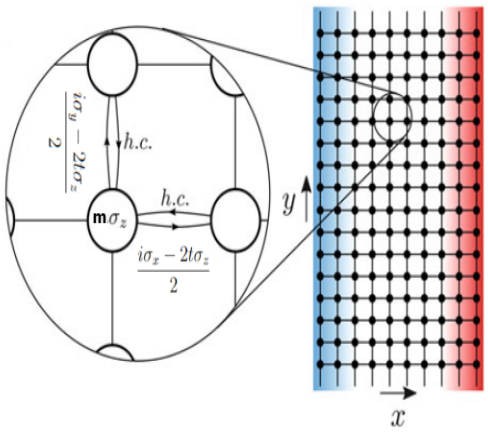

Figure 3.7: Real space picture of the Model

A particle with two internal states hops on a square lattice in this model. Both the onsite potential and the hopping amplitudes are operators that act on the internal states. The illustration portrays a particle with two internal states navigating a lattice, where an operation is associated with the internal degree of freedom during nearest-neighbour hops. Importantly, these operations vary for hops along the x and y directions. The model includes a staggered onsite potential of strength m, with the internal degree of freedom representing two sites within the unit cell. In contrast to the SSH model [6,5],

the real-space expression of the model's Hamiltonian, similar to the QWZ model, lacks intuitive clarity.

Chapter 4

3D Chern Insulator Model

In the preceding section, we delved into the 2D Chern Insulator model, revealing band-insulating states distinguished by a non-zero Chern number. Our attention now turns to assembling 3D Chern models by stacking individual sheets with distinct Chern numbers. This study centres on a detailed examination of the band structure arising from stacking two layers, each endowed with its unique Chern number. The objective is to closely analyze the band properties of this composite model and evaluate the Chern numbers at different planes within the structure.

1 Model Hamiltonian and Energy Bands:

The single-particle Hilbert space of the composite system comprising D layers is formed by the direct sum of the spaces associated with each layer.

$$H_D = H_{L1} \bigoplus H_{L2} ..... \bigoplus H_{LD} \tag{4.1}$$

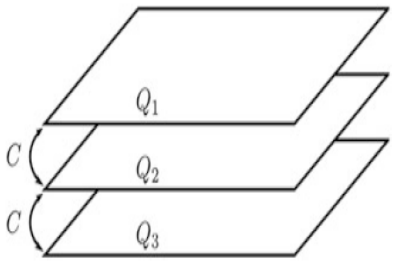

Figure 4.1: Layering Sheets to Construct 3D Model[7]

We will restrict ourselves to stacking two layers with different Chern numbers. When

stacking two layers with different Chern numbers, we essentially create a bilayer system with nontrivial topological properties. The Hamiltonian for such a system can be written as a 2x2 block matrix form.

Let's consider the simplest case of a bilayer system with layers labelled by indices 1 and 2. The Hamiltonian for each layer can be written as:

$$H_{L1}(\mathbf{k}) = \mathbf{d}_1(\mathbf{k}) \cdot \sigma$$

$$H_{L2}(\mathbf{k}) = \mathbf{d}_2(\mathbf{k}) \cdot \sigma$$

The total Hamiltonian for the stacked system is given by:

$$H(\mathbf{k}) = \begin{bmatrix} H_{L1}(\mathbf{k}) & 0 \\ 0 & H_{L2}(\mathbf{k}) \end{bmatrix}$$

In this stacked system, consider interlayer coupling terms that couple the two layers. These terms can be modelled by adding off-diagonal terms to the Hamiltonian:

$$H_{\text{interlayer}}(\mathbf{k}) = \begin{bmatrix} 0 & C(\mathbf{k}) \\ C^\dagger(\mathbf{k}) & 0 \end{bmatrix}$$

where $C(\mathbf{k})$ is the interlayer coupling term. The specific form of $C(\mathbf{k})$ will depend on the details of the system and how the layers are coupled.

So, the total Hamiltonian for the stacked bilayer system with different Chern numbers is the sum of the individual layer Hamiltonians and the interlayer coupling term:

$$H_{\text{total}}(\mathbf{k}) = H(\mathbf{k}) + H_{\text{interlayer}}(\mathbf{k}).$$

Let's delve into the band structure of the simplest case. Given that the Hamiltonian is in block form if we designate C as the null matrix, the eigenvalues of H_{L1} and H_{L2} will precisely be the eigenvalues of the complete Hamiltonian, H. For the purpose of our exploration, we set k_z to zero while varying u ($= \frac{m_1}{t_1}$) and v ($= \frac{m_2}{t_2}$).

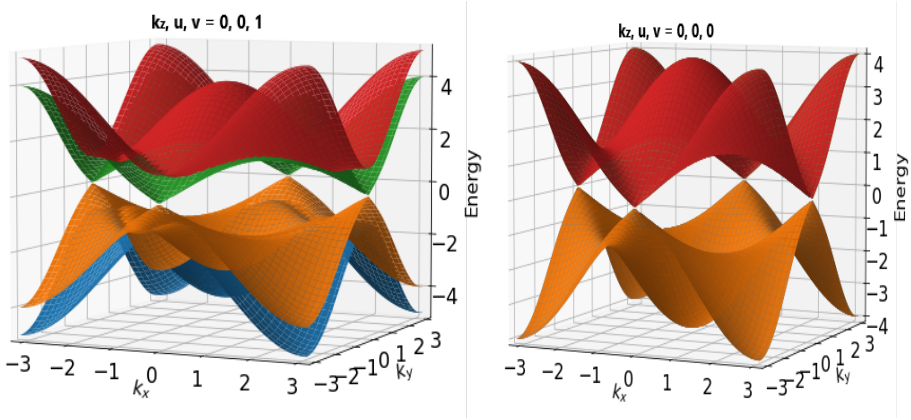

Figure 4.2: Band structure at $k_z = 0$ and two different parameters of u and v

Upon examination of the figure, a distinct pattern emerges: when (u, v) takes on values of 0 or 1, four distinct bands and four Dirac points become apparent. This scenario aligns with our familiar 2D case, where for u or v equal to 0, ± 4, Dirac points are expected. Interestingly, only two bands with four Dirac points are observed when (u, v) equals 0, 0. This is because the upper two and lower two bands essentially overlap.

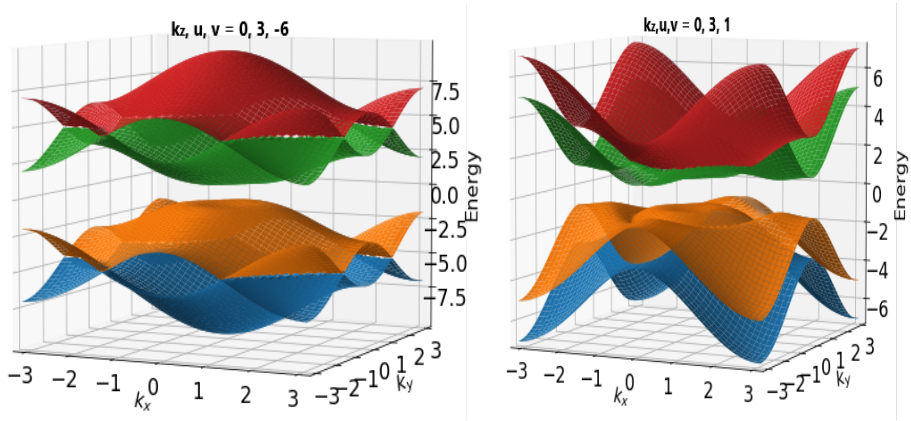

Figure 4.3: Band structure at $k_z = 0$ and two different parameters of u and v

However, a gapped spectrum unfolds in other cases, as depicted in the accompanying figure. It's noteworthy that although we have chosen a specific value for k_z in the plotting process, the band structure remains invariant for any k_z values. This constancy is a consequence of C being a null matrix.

Since each site comprises two orbitals, let's construct the band structure by conferring the freedom of hopping exclusively within the up orbital along the z-direction with hopping amplitude 'a'. All other potential hopping interactions are set to zero in this context.

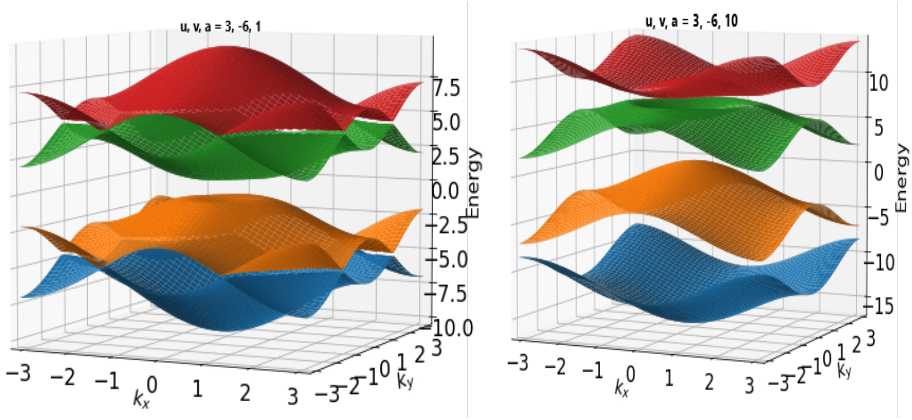

Figure 4.4: Band structure for up to up hopping along z direction

Let's generate the band structure by allowing hopping from up to down orbital along the z-direction with hopping amplitude 'b'. All other potential hopping interactions are nullified for this analysis.

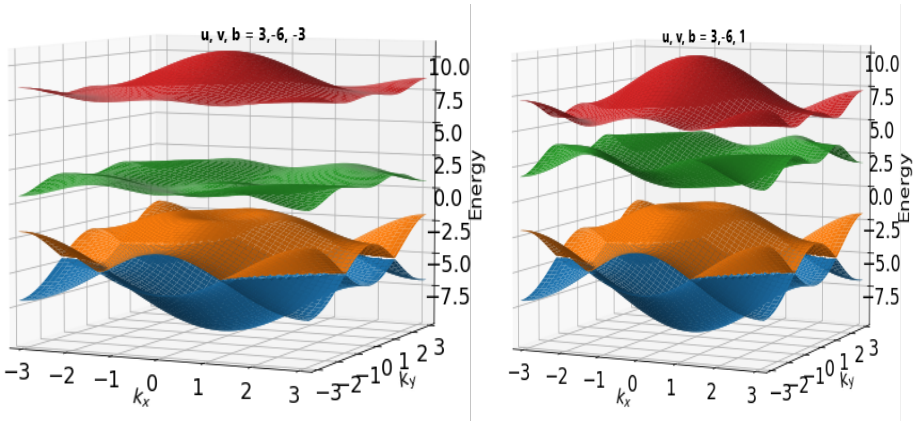

Figure 4.5: Band structure for up to down hopping along z direction

Likewise, we can visualize the band structure by manipulating k_x and k_y, while keeping the other two momentum indices fixed. (Refer to the figure below for illustration.)

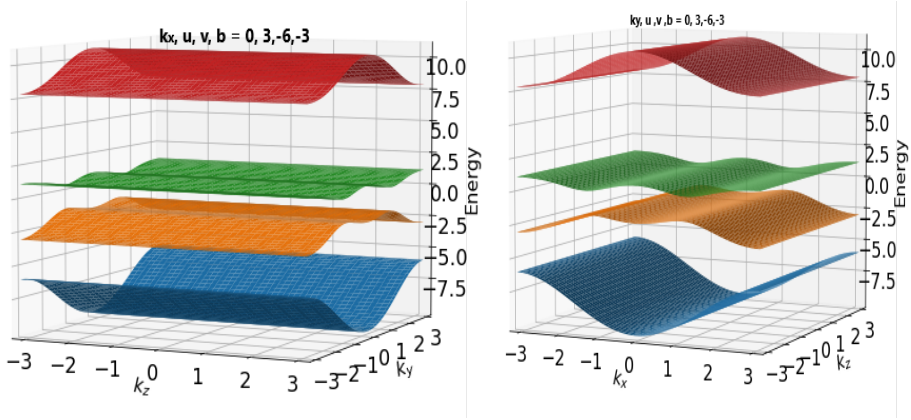

Figure 4.6: Band structure in k_z - k_y plane and k_z - k_x plane for various parameters

2 Chern Number at Different Planes:

Let's delve into the discussion of the Chern number for our stacked Hamiltonian under the constraint of exclusively allowing up-to-down hopping, with a specified hopping amplitude 'b'. We will analyze the Chern number of the system in the k_x - k_y, k_x - k_z, and k_y - k_z planes.

Let's begin the analysis of the system with real hopping. We compute the Chern number of the ground energy level while varying the hopping amplitude 'b' for three distinct cases:

- In the first case, we set the 1st sheet in a topological state (with 'u' taking any value between -4 to 4) and the 2nd sheet in a trivial state (with 'v' taking any value outside the range -4 to 4).
- In the second case, both sheets are placed in topological states (with both 'v' and 'u' lying between -4 to 4).
- In the third case, the 1st sheet is in a trivial state (with 'u' taking any value outside -4 to 4), and the 2nd sheet is in a topological state (with 'v' taking any value outside the range -4 to 4).

Analyzing these scenarios will provide insights into the system's behaviour under different configurations of the hopping amplitudes.

Let's examine the Chern number for the lower band in the $k_x - k_y$ plane, depicted in the figure below. We will analyze its behaviour as a function of the parameter b for the three distinct cases mentioned earlier.

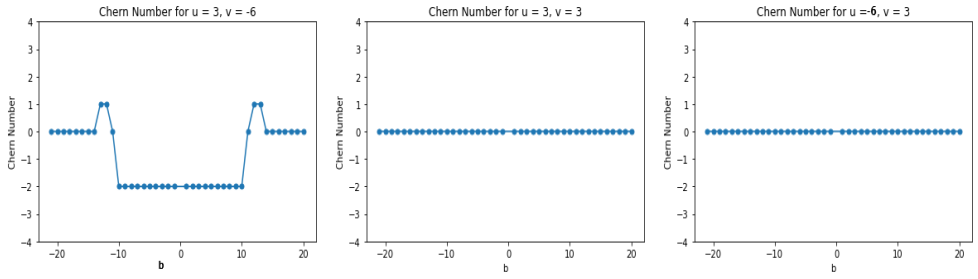

Figure 4.7: Chern number in the k_x-k_y plane for different cases as a function of b.

Similarly, in $k_x - k_z$ plane,

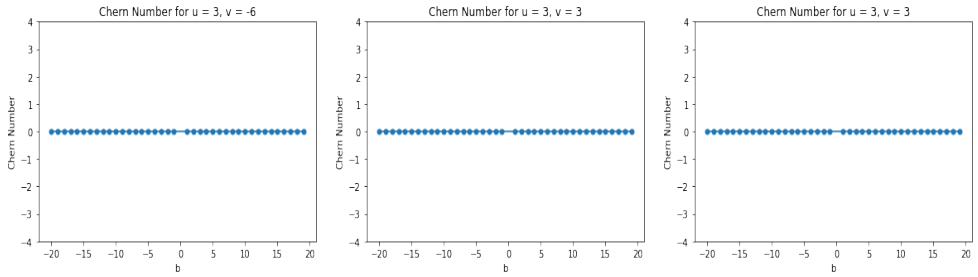

Figure 4.8: Chern number in the k_x-k_z plane for different cases as a function of b.

Similarly, in $k_y - k_z$ plane,

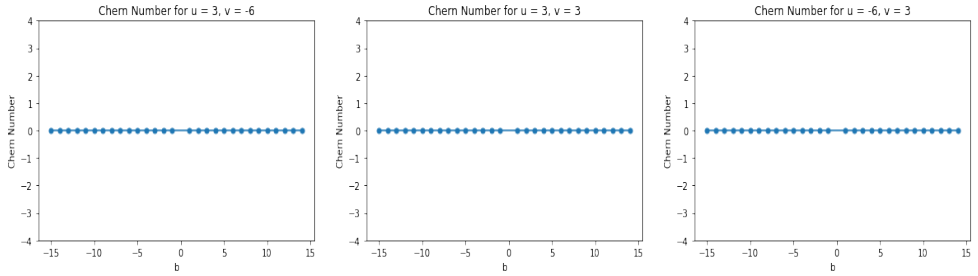

Figure 4.9: Chern number in the k_y-k_z plane for different cases as a function of b.

Now, let us plot the Chern Number for higher bands in $k_x - k_y$ plane,

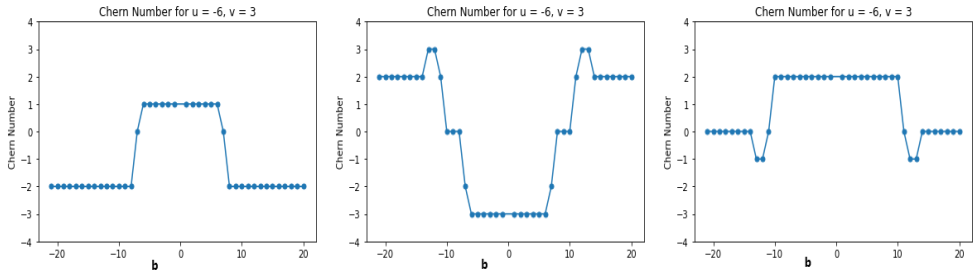

Figure 4.10: Chern number in the k_y-k_z plane for 1st, 2nd & 3rd excited states

Chapter 5

Conclusion

We commence with an examination of the Berry curvature and its correlation with the Kubo formula. Subsequently, we formalize the Chern Insulator Model, computing both the band structure and the emergence of non-trivial insulating states within the system. Our exploration advances as we assemble a 3D model by stacking 2D Chern Models. The band structure and Chern numbers are computed across various Hamiltonian parameters. Concluding our discussion, we illustrate a transition from a trivial to a topological phase, discernible in the different bands with respect to up and down hopping along the z-direction.

Chapter 6

Appendix

1 Sternhiemer Equation

Lets assume Hamilton and its eigenvalues and eigenstates are function of some parameter λ,Then we can write the time-independent Schrodinger equation

$$H(\lambda)\left|n(\lambda)\right\rangle = E_n(\lambda)\left|n(\lambda)\right\rangle \tag{6.1}$$

Differentiating the whole equation,Note the dependence on λ is not shown for the follwing equation

$$\partial_\lambda(H - E_n)\left|n\right\rangle = (E_n - H)\left|\partial n\right\rangle \tag{6.2}$$

By hitting the above equation with $\langle n|$, we get

$$\partial_\lambda E_n(\lambda) = \langle n|\,\partial_\lambda H\left|n\right\rangle \tag{6.3}$$

Putting this in equation 6.2 we get

$$(E_n - H)\left|\partial n\right\rangle = \partial_\lambda H\left|n\right\rangle - \left|n\right\rangle\langle n|\,\partial_\lambda\left|n\right\rangle \tag{6.4}$$

Let $1 - \left|n\right\rangle\langle n| = Q_n$, we get the sternhiemer equation

$$(E_n - H)\left|\partial n\right\rangle = Q_n\left|\partial n\right\rangle \tag{6.5}$$

The solution of **sternhiemer equation** are as follows, it can be checked by putting this experssion back in the equation.

$$|\partial_\lambda n\rangle = -iA_n |n\rangle + \sum_{n\neq m} \frac{|m\rangle \langle m|}{E_n - E_m} \partial_\lambda H |n\rangle \tag{6.6}$$

We can find the A by hitting the above equation by $\langle n|$

$$A_n = i \langle n|\partial_\lambda n\rangle \tag{6.7}$$

Thus A is the berry connection in the above equation,rearranging the above equation as follows

$$|\partial_\lambda n\rangle + iA_n |n\rangle = T_n(\partial_\lambda H) |n\rangle \tag{6.8}$$

where $T_n = \sum_{n\neq m} \frac{|m\rangle\langle m|}{E_n - E_m}$

$$Q_n |\partial_\lambda n\rangle = T_n(\partial_\lambda H) |n\rangle \tag{6.9}$$

The above relation relates parameter derivative of Hamilton with derivatives of its eigenstates which will be used in expressing the conductivity in terms of Berry Curvature

2 Two Level System

Two-level systems (or two-state systems) are very important simple quantum systems that can exist in any quantum superposition of two independent quantum states. In many cases, we can use some approximation to simplify the problem and change it into a two-level system. The Hamiltonian of any two-level system can be written in the form

$$H = \begin{pmatrix} a & b \\ c & d \end{pmatrix} \tag{6.10}$$

Since $H^\dagger = H$ i.e. a & d are real numbers and $b^* = c$. The characteristics equation is

$$Det(H - \lambda I) = 0$$

The solution of the above equation will be of the form,

$$\lambda = \frac{(a+d)}{2} \pm \sqrt{(a-d)^2 + 4|b|^2}, \qquad (\because\ b^* = c) \tag{6.11}$$

Therefore, the two energy eigenvalues of the system are $E_+ = \frac{(a+d)}{2} + \sqrt{(a-d)^2 + 4|b|^2}$ and $E_- = \frac{(a+d)}{2} - \sqrt{(a-d)^2 + 4|b|^2}$. And they will degenerate ($E_+ = E_-$) if a = d and b = c = 0.

We know that any 2×2 matrix can be represented by Pauli matrices (σ_0, σ_1, σ_2, σ_3)[1]. So, the Hamiltonian of the 2-level system is

$$H = d_0\sigma_0 + d_1\sigma_1 + d_2\sigma_2 + d_3\sigma_3 = \begin{pmatrix} d_0 + d_3 & d_1 - id_2 \\ d_1 + id_2 & d_0 - d_3 \end{pmatrix} \tag{6.12}$$

Since $H^\dagger = H$ i.e. d_0, d_1, d_2, d_3 are real numbers. By solving the eigenvalue equation, the eigenvalue of the above Hamiltonian will be of the form,

$$\lambda = d_0 \pm \sqrt{d_1^2 + d_2^2 + d_3^2} \tag{6.13}$$

Let us find out the eigenstates of the Hamiltonian. Let $|\Psi_\pm\rangle$ be the eigenstate of $\lambda_\pm$. So, the eigenvalue equation will be of the form

$$(d_0\sigma_0 + d_1\sigma_1 + d_2\sigma_2 + d_3\sigma_3)\,|\Psi_\pm\rangle = \lambda_\pm\,|\Psi_\pm\rangle$$

Let us define $\vec{d} = (d_1, d_2, d_3)$ and $\vec{\sigma} = (\sigma_1, \sigma_2, \sigma_3)$.Then, the above equation will be of the form

$$\vec{d} \cdot \vec{\sigma} \left|\Psi_{\pm}\right\rangle = (\lambda_{\pm} - d_0) \left|\Psi_{\pm}\right\rangle = C_{\pm} \left|\Psi_{\pm}\right\rangle \qquad (\because\ \sigma_0 = I_{2\times 2}) \tag{6.14}$$

Explicitly, the above equation will be

$$\begin{pmatrix} d_3 & d_1 - id_2 \\ d_1 + id_2 & -d_3 \end{pmatrix} \begin{pmatrix} |\Psi_{1\pm}\rangle \\ |\Psi_{2\pm}\rangle \end{pmatrix} = C_{\pm} \begin{pmatrix} |\Psi_{1\pm}\rangle \\ |\Psi_{2\pm}\rangle \end{pmatrix} \tag{6.15}$$

Let us make a change of variable $(d_1, d_2, d_3) \longrightarrow (d, \theta, \phi)$ such that $d_1 = d\sin\theta\cos\phi$, $d_2 = d\sin\theta\sin\phi$, $d_3 = d\cos\theta$ and d = $\sqrt{d_1^2 + d_2^2 + d_3^2}$

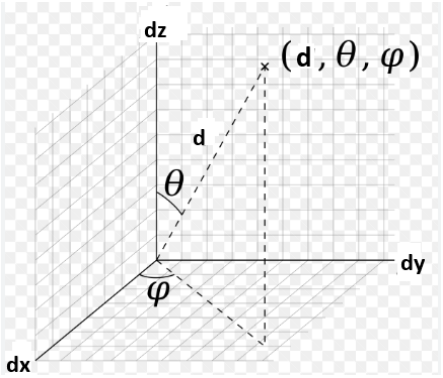

Figure 6.1: **Schematics of Co-ordinate Transformation**

In the new coordinate, the eigenvalue equation will be,

$$\begin{pmatrix} d\cos\theta & e^{-i\phi} d\sin\theta \\ e^{i\phi} d\sin\theta & -d\cos\theta \end{pmatrix} \begin{pmatrix} |\Psi_{1\pm}\rangle \\ |\Psi_{2\pm}\rangle \end{pmatrix} = \pm d \begin{pmatrix} |\Psi_{1\pm}\rangle \\ |\Psi_{2\pm}\rangle \end{pmatrix} \tag{6.16}$$

Let us first solve for positive eigenvalue or $|\Psi_+\rangle$ state. Then, the above equation will be

$$\begin{pmatrix} d\cos\theta & e^{-i\phi} d\sin\theta \\ e^{i\phi} d\sin\theta & -d\cos\theta \end{pmatrix} \begin{pmatrix} |\Psi_{1+}\rangle \\ |\Psi_{2+}\rangle \end{pmatrix} = d \begin{pmatrix} |\Psi_{1+}\rangle \\ |\Psi_{2+}\rangle \end{pmatrix}$$

The above equation will give us the condition,

$$\sin\frac{\theta}{2} \left|\Psi_{1+}\right\rangle = e^{-i\phi} \cos\frac{\theta}{2} \left|\Psi_{2+}\right\rangle \implies \left|\Psi_+\right\rangle = \begin{pmatrix} \cos\frac{\theta}{2} \\ e^{i\phi}\sin\frac{\theta}{2} \end{pmatrix} \tag{6.17}$$

Similarly, we can solve for negative eigenvalue (-d) $|\Psi_-\rangle$ state and then will get

$$\cos\frac{\theta}{2}|\Psi_{1-}\rangle = -e^{-i\phi}\sin\frac{\theta}{2}|\Psi_{2-}\rangle \implies |\Psi_-\rangle = \begin{pmatrix} -e^{-i\phi}\sin\frac{\theta}{2} \\ \cos\frac{\theta}{2} \end{pmatrix} \tag{6.18}$$

Using these two eigenstates we can derive the general relation of Berry curvature for two-level systems

$$|\Psi_+\rangle = \begin{pmatrix} \cos\frac{\theta}{2} \\ e^{i\phi}\sin\frac{\theta}{2} \end{pmatrix} |\Psi_-\rangle = \begin{pmatrix} -e^{-i\phi}\sin\frac{\theta}{2} \\ \cos\frac{\theta}{2} \end{pmatrix}$$

We first calculate the berry potential and then take its curl to find the Berry curvature

$$\nabla|\psi+\rangle = \frac{\partial|\psi+\rangle}{\partial d}\hat{d} + \frac{1}{d}\frac{\partial|\psi+\rangle}{\partial\theta}\hat{\theta} + \frac{1}{dsin(\theta)}\frac{\partial|\psi+\rangle}{\partial\phi}\hat{\phi} \tag{6.19}$$

$$= \frac{1}{d}\begin{pmatrix} -(1/2)sin(\theta/2) \\ (1/2)e^{i\phi}cos(\theta/2) \end{pmatrix}\hat{\theta} + \frac{1}{dsin(\theta)}\begin{pmatrix} 0 \\ ie^{i\phi}sin(\theta/2) \end{pmatrix}\hat{\phi}$$

$$\langle\psi+|\nabla|\psi+\rangle = \frac{1}{2d}[2i\frac{sin^2(\theta/2)}{sin(\theta)}\hat{\phi} = i\frac{sin^2(\theta/2)}{dsin(\theta)}\hat{\phi} \tag{6.20}$$

From this, we get the berry curvature to be

$$\nabla\times\langle\psi+|\,i\nabla|\psi+\rangle = \frac{1}{dsin(\theta)}\frac{\partial}{\partial\theta}[sin\theta\frac{isin^2(\theta/2)}{dsin(\theta))}]\hat{d} = -\frac{\hat{d}}{2d^2} \tag{6.21}$$

The above result is for $|\phi+\rangle$ state for the other eigenstate it will be of oposite sign making the total berry curvature integrated over all bands zero.In real system not all bands are occupied at thermal equilibrium with surrounding leading to finite berry curvature and topology in materials.

3 Kramer's Theorem

It states when Time reversal symmetry is present in the system and spin of electrons is taken into account then all the energy eigenvalues as at least two -fold degenerate.
Proof: Suppose $|u\rangle$ is a non degenerate eigenvector of H with eigenvalue E.Let $|v\rangle = T|u\rangle$ as [TH] = 0 we can show that

$$H(T|u\rangle) = TH|u\rangle = E(T|u\rangle) \tag{6.22}$$

thus $T|u\rangle = v$ is also an eigenstate of H as $|u\rangle$ is non-degenerate we expect

$$|v\rangle = e^{i\phi}|u\rangle \tag{6.23}$$

but for a spin half system $T^2 = -1$

$$T^2|u\rangle = Te^{i\phi}|u\rangle = e^{i\phi}T|u\rangle = |u\rangle \tag{6.24}$$

This is a contradiction hence our assumption is wrong thus under TRS $|u\rangle$ and $|v\rangle$ are degenerate.For lattice system it transforms into following relation.

$$T|\psi_{n,-k}\rangle = |\psi_{n,k}\rangle \tag{6.25}$$

$$\gamma_n = \oint \langle\psi|\nabla\psi\rangle .dR \tag{6.26}$$

Acknowledgement

I express profound gratitude to my supervisor, Dr. Kush Saha, whose unwavering guidance introduced me to the enthralling realm of theoretical condensed matter physics. His brilliance, extensive knowledge, and fervour for the subject have consistently motivated me throughout this project.

In addition, I extend my sincere acknowledgement to my dedicated project partner, Dikkar Shubhay, for his invaluable assistance and engaging discussions related to the project. I would also like to express my appreciation to Ivan Dutta Bhaiya for his wholehearted encouragement and guidance.

Special thanks go to Hirnamay Das Bhiaya for his assistance in coding for the 3D Chern Insulator and to Sarbajit and Aditya Bhaiya for addressing my doubts regarding the project.

Last but certainly not least, my heartfelt thanks go to my friends, fellow course students, and all those who provided mental and physical support throughout this project. Their contributions have served as the bedrock of my strength during this endeavour. I am genuinely humbled and privileged to have been surrounded by such exceptional individuals and resources. Words alone cannot adequately convey my gratitude for their unwavering support.

Chapter 7

References

1. B. Zwiebach, Lecture Notes, MIT OCW, *Spin One-Half, Bras, Kets, And Operators*, September 17, 2013.

2. Xiao-Liang Qi, Yong-Shi & Shou-Cheng Zhang, *Topological quantization of the spin Hall effect in two-dimensional paramagnetic semiconductors*, Phys. Rev. B 74, 085308, 10 August 2006

3. Gui-Geng Liu, Peiheng Zhou, Yihao Yang, Haoran Xue, Xin Ren, Xiao Lin, Hong-Xiang Sun, Lei Bi, Yidong Chong & Baile Zhang, *Observation of an unpaired photonic Dirac point*, Nature Communications volume 11, Article number: 1873 (2020).

4. David Tong, *Quantum Hall Effect, Lecture Notes, 2016*

5. Navketan Batra & Goutam Sheet, *Understanding Basic Concepts of Topological Insulators Through Su-Schrieffer-Heeger (SSH) Model, arXiv:1906.08435, 2019*

6. W. P. Su, J. R. Schrieffer, & A. J. Heeger, *Solitons in Polyaeetylene, Physical Review Letters, Volume 42, Number 25*

7. J. K. Asboth, L. Oroszlany and A. Palyi, *A Short Course on Topological Insulators, arXiv:1509.02295, 2015*

8. David Vanderbilt, *Berry phases in electronic structure theory: electric polarization, orbital magnetization and topological insulators*, 26 October 2018